

Study of Deprotection Reaction during Exposure in Chemically Amplified Resists for Lithography Simulation

Yasuhiro Miyake, Mariko Isono and Atsushi Sekiguchi

Litho Tech Japan Corporation, 2-6-6-201, Namiki, Kawaguchi, Saitama 332-0034, Japan

Deprotection reactions of chemically amplified resists during exposure are observed by using the *in-situ* FT-IR with the 248nm light source, and resist profiles are simulated using the activation energy and the prefactor calculated. The resists used in this experiment are poly(*p*-hydroxystyrene) (PHS) protected by Ethoxyethyl (EOE) group, by *tert*-Butoxycarbonyl (t-BOC) group and by these heterogeneous protection groups. The activation energy for the EOE resist is much lower than that for the t-BOC resist. The existence of heterogeneous protection groups affect mutually deprotection reactions; the EOE group additions to t-BOC resist reduce the activation energy for the deprotection reaction of t-BOC group. It is confirmed that existences of heterogeneous protection groups affect the formation of resist pattern profile by lithography simulator.

Keywords: deprotection reaction, CA resist, activation energy, simulation

1. INTRODUCTION

Beginning with the study by Ito et al. in 1987^[1], chemically amplified (CA) resists using acid catalyzed reactions have become indispensable for manufacturing sub-half micron semiconductor devices. During this period, various studies have been performed to improve the resolution of CA resists and to improve environmental stability^{[2]-[5]}. In positive-type CA resists, acid is produced by catalysis in photochemical reactions, and protection groups are dissociated in the heating process (PEB: post exposure bake) that follows exposure. Therefore the acid generation efficiency, the acid diffusion, the type of protection groups and the protection ratios are closely related to CA resist performance. Clearing of deprotection reactions is essential for the development of resists and the evaluation of process. In recent years, appropriate models for deprotection reactions during PEB have been proposed^{[6]-[8]}. However there have been few reports of analysis of deprotection reactions during exposure^[9]. Therefore we use an FT-IR spectrometer equipped with a UV light source, analyze and model of deprotection reactions during exposure in positive-type CA resists. In addition to determining the parameters for lithography simulation, we simulate the resist profiles.

2. EXPERIMENTAL

The analysis system used in this experiment was the MODEL PAGA-100 by Litho Tech Japan (Fig. 1).

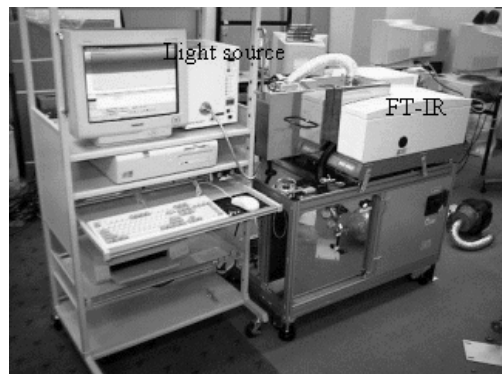


Fig. 1 External view of the MODEL PAGA-100

This system was based on a standard FT-IR spectrometer, but equipped with a light source, a bake plate and a wafer transport shuttle in the sample chamber (Fig. 2). The exposure light used a dielectric film filter to narrow the spectral bandwidth to 248 nm from a VU-rays of Xe-Hg lamp. Exposure power in wafer surface was 3 mW/cm².

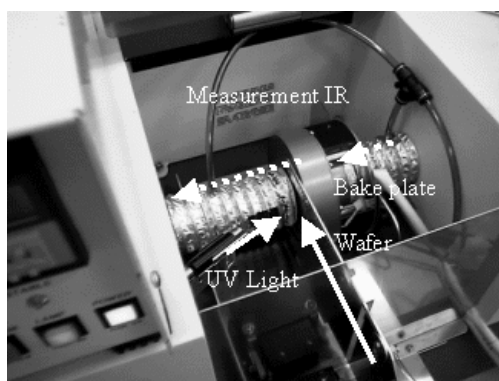


Fig. 2 Internal view of the MODEL PAGA-100 sample chamber

The bake plate was used to control the ambient temperature during exposure from room temperature to 150 °C. In order to enable *in-situ* observations of IR-rays through a Si wafer, a 10 mm diameter hole was punched in the center of the bake plate. In measurement, at first a sample was inserted into the sample chamber by a wafer transport shuttle, started exposure and measurement as soon as sample reached the set temperature by the bake plate.

The resists used in this experiment were composed of PHS protected by EOE group or by t-BOC group, and by these heterogeneous protection groups (Fig. 3). Table 1 shows the resists composition.

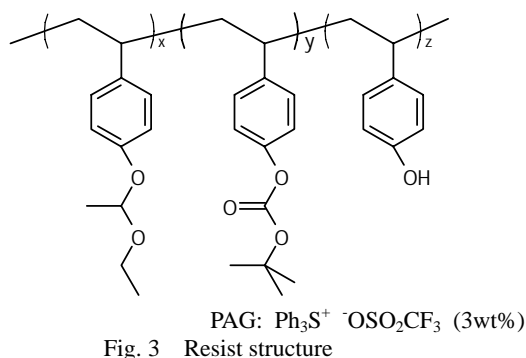


Table 1 Resists composition

	EOE(x)	t-BOC(y)	OH(z)
H450055	45%	0%	55%
C260965	26%	9%	65%
C122365	12%	23%	65%
H003565	0%	35%	65%

The homopolymer resist used was PHS protected by 45 % EOE group, (named H450055, numbers are the protection percentage of EOE, t-BOC, and OH group), or by 35 % t-BOC group (H003565). The copolymer resist used was PHS protected by 26 % EOE group and by 9 % t-BOC group

(C260965), or protected by 12 % EOE group and by 23 % t-BOC group (C122365). Triphenyl sulphonium triflate was used at 3 wt% into the resists as a photo acid generator (PAG).

The resists were spin-coated at 1 μm thickness on Si wafer for all samples, and were prebaked at 90 °C for 90 s. These samples were exposed in the sample chamber during exposure varied, and *in-situ* measurements of the IR spectra were performed. The decreases of characteristic absorption obtained from *in-situ* measurements were converted to deprotection reaction curves. The deprotection reaction curves were fitted by exponential functions as the deprotection reaction constant C_2 [cm^2/mJ]. The activation energy E_a [kJ/mol] and the prefactor $\ln(A_r)$ [s^{-1}] were calculated from an Arrhenius plot of C_2 , and compared. A sequence of analyses was calculated by the Deprotection Simulator software^[8,9].

The other parameters for lithography simulations were determined by the development rate measurement system RDA-790 and the ABC parameter analyzer MODEL-400^[10].

3. Deprotection Reaction Model

The EOE resist generates the acid by exposure. The acid is amplified by heat reaction of PEB. It causes the deprotection reaction of EOE group. The dissociated EOE group undergoes hydrolysis and decomposes to ethanol and aldehyde (Fig. 4a)^[11]. The t-BOC resist generates the acid by exposure. The acid is amplified by heat reaction of PEB. It causes the deprotection reaction of t-BOC group. The dissociated t-BOC group decomposes to carbon dioxide and isobutene (Fig. 4b)^[1, 12].

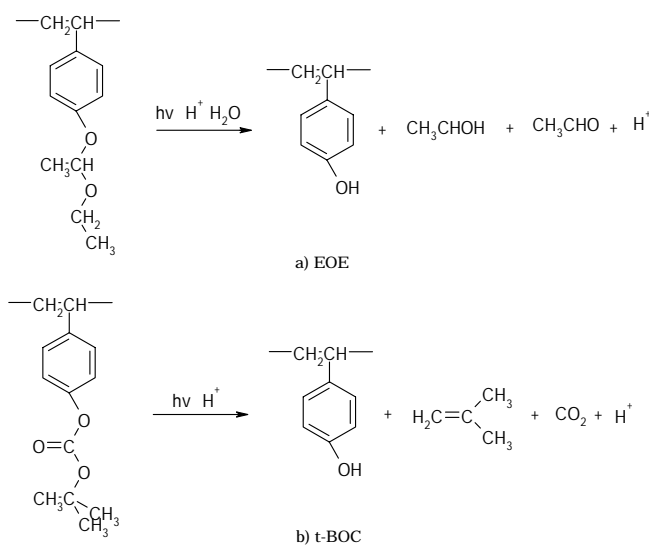


Fig. 4 Deprotection reaction mechanism

4. RESULTS

4.1 Measurement Results

Fig. 5 shows C260965 *in-situ* IR spectra from deprotection during exposure of EOE group and t-BOC group at 68 °C.

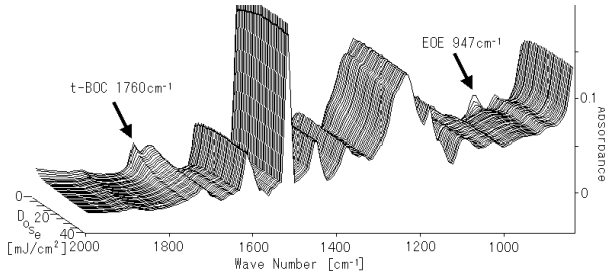


Fig. 5 IR absorption spectra of C260965 at 68°C

As the exposure dose increased, characteristic absorption of ether groups at 947 cm⁻¹ decreased in the EOE group, and of ester carbonyl groups at 1760 cm⁻¹ decreased in the t-BOC group. The characteristic absorption was standardized as protection ratio.

Fig. 6 shows protection ratio of PHS versus exposure dose.

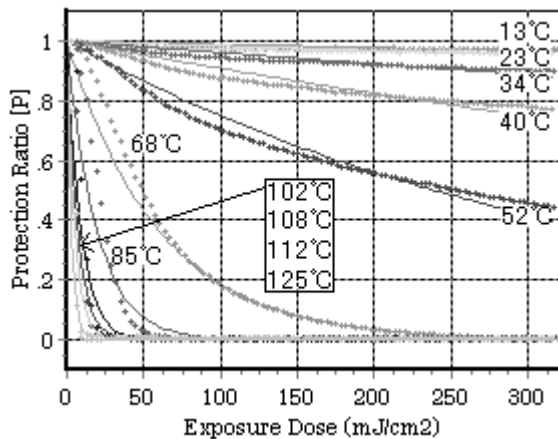


Fig. 6 Protection ratio vs. exposure dose for t-BOC group

Deprotection reaction occurred with increase in the exposure ambient temperature, and an exponential function was fitted to the deprotection reaction curve (Eq. 1).

$$[P]_{\text{exp}} = \exp(-C_2 E) \quad (\text{Eq. 1})$$

where $[P]_{\text{exp}}$ is the protection ratio, C_2 is the deprotection reaction constant, and E is the exposure dose.

Fig. 7 shows Arrhenius plots of deprotection reaction constant C_2 , calculated from Eq. 1 for the several samples with the exposure ambient temperature varied.

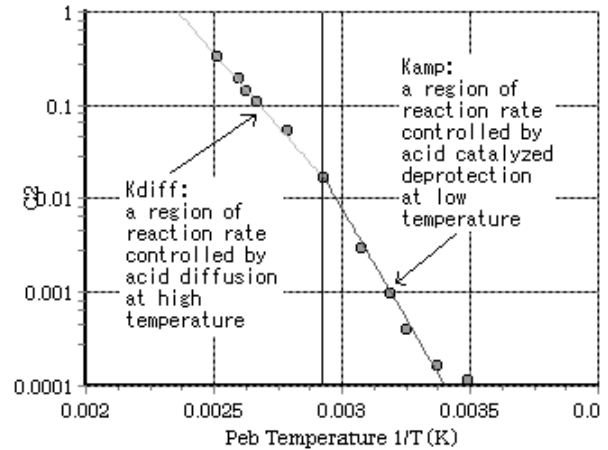


Fig. 7 Arrhenius plot of deprotection reaction constant C_2 for t-BOC group

Eq. 2 shows the Arrhenius formula.

$$C_2 = A_r \exp(-E_a / RT) \quad (\text{Eq. 2})$$

where C_2 is the deprotection reaction constant, A_r is the prefactor, E_a is the activation energy, R is the universal gas constant, and T is the absolute temperature.

Existence of different two regions was found by the activation energies calculated from Arrhenius plots; a region of reaction rate controlled by acid catalyzed deprotection at low temperature (K_{amp}), a region of reaction rate controlled by acid diffusion at high temperature (K_{diff}). The existence of two regions in the activation energy agreed with the model proposed by Byers and Petersen et al.^[13, 14]

Fig. 8 shows protection ratio versus exposure dose for EOE group at 23 °C.

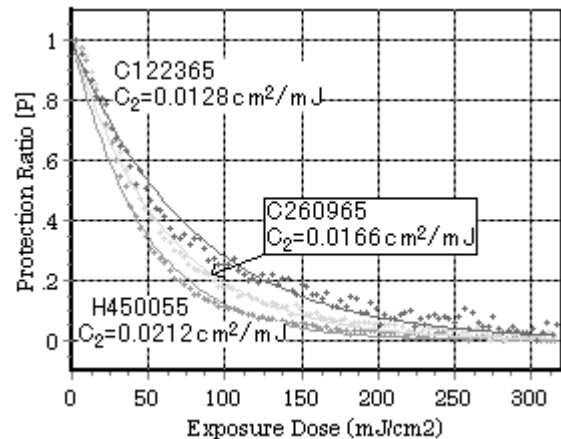


Fig. 8 Protection ratio vs. exposure dose for EOE group at 23 °C

Deprotection reaction curves of EOE group became smooth by introducing t-BOC group. Fig. 9 shows protection ratio versus exposure dose for t-BOC group at 68 °C.

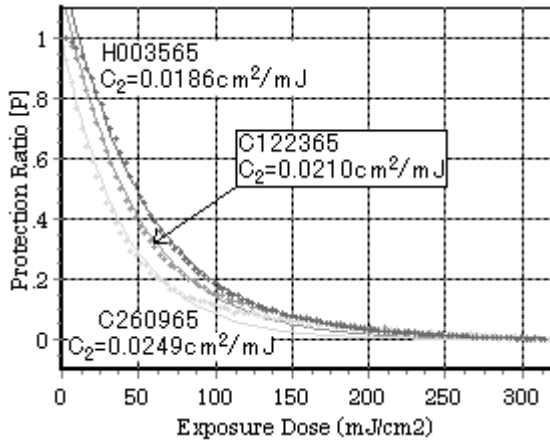


Fig. 9 Protection ratio vs. exposure dose for t-BOC group at 68 °C

Deprotection reaction curves of t-BOC group became sharp by introducing EOE group. It was found that existence of heterogeneous protection groups affected the action of acid on deprotection reaction.

Table 2 shows the activation energies E_a and the prefactors $\ln(A_r)$.

Table 2 Activation energies and prefactors

		H450055	C260965	C122365	H003565
EOE	$K_{amp}E_a$ [kJ/mol]	37.24	43.09	45.44	-
	$K_{amp}\ln(A_r)$ [s ⁻¹]	11.26	13.34	14.06	-
	$K_{diff}E_a$ [kJ/mol]	10.38	15.77	18.03	-
	$K_{diff}\ln(A_r)$ [s ⁻¹]	1.10	3.07	3.76	-
t-BOC	$K_{amp}E_a$ [kJ/mol]	-	51.46	67.24	98.95
	$K_{amp}\ln(A_r)$ [s ⁻¹]	-	14.31	19.53	30.80
	$K_{diff}E_a$ [kJ/mol]	-	28.12	34.69	44.14
	$K_{diff}\ln(A_r)$ [s ⁻¹]	-	6.72	8.69	11.94

The activation energies were compared at low temperature region. The activation energy for EOE group deprotection reaction ($K_{amp}E_a$ of H450055) was 37.24 kJ/mol, while for t-BOC group deprotection reaction ($K_{amp}E_a$ of H003565) was 98.95 kJ/mol. The activation energy for EOE resist was much lower than that for t-BOC resist. Progress of the deprotection reaction in EOE resist during exposure at room temperature could be explained in terms of difference in activation energies. In the copolymer resist, introduction of EOE group into

PHS protected by t-BOC group resulted in decrease of the activation energy required for the t-BOC group deprotection reaction. It was found that existence of heterogeneous protection groups affected the action of acid on deprotection reaction, too.

4.2 Simulation Results

Table 3 shows the used parameters in simulations. Resist profiles were simulated with the exposure ambient temperature varied using the activation energies and the prefactors shown in section 3.2 (Figs. 10 and 11).

Table 3 used parameters in simulations

Parameters	Values
Resist Thickness	700 nm
Prebake	90 °C / 90 s
A	-0.03 μm^{-1}
B	0.24 μm^{-1}
C	0.04 cm^2/mJ
Development Time	60 s
Development Model	Mack
Development R_{max}	308 nm/s
Development R_{min}	0.11 nm/s
Development M_{th}	0.01
Development n	8
Exposure Wavelength	248 nm
Feature Width	250 nm L/S

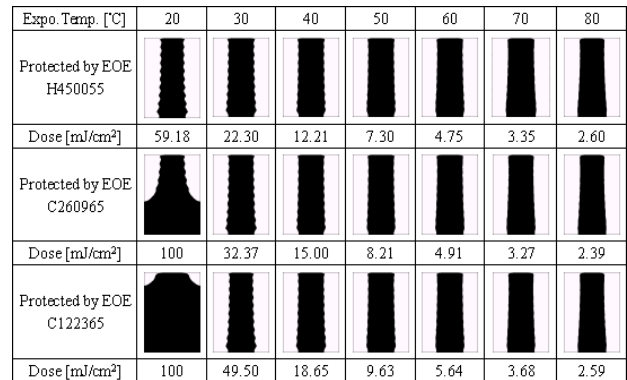


Fig. 10 Simulation results (250nm L/S) for PHS resist protected by EOE group

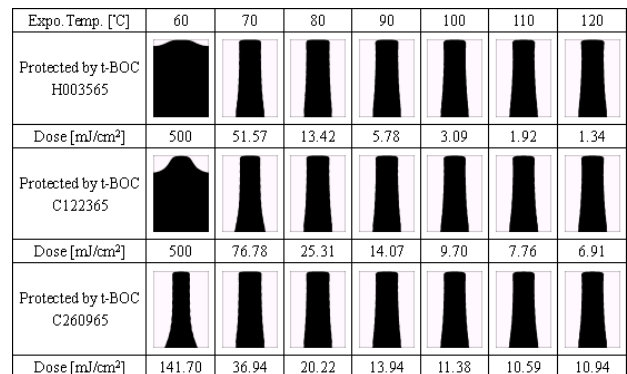


Fig. 11 Simulation results (250nm L/S) for PHS resist protected by t-BOC group

The simulations were performed focusing on the activation energies and the prefactors for each protection groups. In the case of the PHS protected by EOE group, 250 nm L/S were patterned at an exposure ambient temperature of 20 °C. However, as the activation energy and the prefactor were increased by introduction of t-BOC group, the optimum exposure dose and the exposure ambient temperature increased. In the case of the PHS protected by t-BOC group, 250 nm L/S were patterned at an exposure ambient temperature of 70 °C. However, the activation energy and the prefactor were increased by introduction of EOE group, with the result that the optimum exposure dose and the exposure ambient temperature were decreased.

It was confirmed that existence of heterogeneous protection groups affected the formation of resist pattern profile.

5. CONCLUSION

Until now, the deprotection reaction is observed by sift of characteristic absorption during PEB. However, it is difficult to accurately analyze deprotection reactions at the protection groups like EOE group dissociated at room temperature. But by using this system for the *in-situ* analysis of deprotection reactions during exposure with the exposure ambient temperature varied, it is possible to obtain valuable insights for deprotection reactions in resists having protection groups which undergo deprotection at room temperatures. In order to clarify change in resist profiles by deprotection reactions during exposure, lithography

simulation studies which take into consideration the activation energies of heterogeneous protection groups will be needed.

REFERENCES

- [1] H. Ito and C. G. Wilson, *ASC Symp. Ser.* **2**, (1984), 11.
- [2] J. V. Crivello and J. H. W. Lam, *Macromolecules*, **10**, (1977), 1307.
- [3] R. A. Ferguson, C. A. Spence, E. Reichmanis, L. F. Thompson and A. R. Neureuther, *Proc. SPIE*, **1262**, (1990), 412.
- [4] G. Pawlowski, R. Dammel and C. R. Lindley, *Proc. SPIE*, **1925**, (1993), 213.
- [5] R. D. Allen, I. Y. Wan, G. M. Wallraff, R. A. Dipietro and D. C. Hofer, *J. Photopolym. Sci. Technol.*, **8**, (1995), 623.
- [6] T. Ohfuji, A. G. Timko, O. Nalamasu and D. R. Stone, *Proc. SPIE*, **1925**, (1993), 213.
- [7] T. Ohfuji, K. Nakano, K. Maeda and E. Hasegawa, *J. Vac. Sci. Technol.*, **13**, (1995), 3022.
- [8] A. Sekiguchi, C. A. Mack, M. Isono and T. Matsuzawa, *Proc. SPIE*, **3678**, (1999), 985.
- [9] A. Sekiguchi, Y. Miyake and M. Isono, *Jpn. J. Appl. Phys.*, **39**, (2000), 1392.
- [10] A. Sekiguchi, C. A. Mack, Y. Minami and T. Matsuzawa, *Proc. SPIE*, **2725**, (1996), 49.
- [11] C. Mertesdorf, N. Munzel, H. Holzwarth, P. Falcigno, H. Schacht, O. Rohde and R. Schulz, *Proc. SPIE*, **2438**, (1995), 84.
- [12] H. Ito and C. G. Wilson, *Polym. Eng. Sci.*, **23**, (1983), 1012.
- [13] J. S. Petersen, C. A. Mack, J. W. Thackeray, R. Sinta, T. H. Fedynyshyn, J. M. Mori, J. D. Byers and D. A. Miller, *Proc. SPIE*, **2438**, (1995), 153.
- [14] J. S. Petersen, C. A. Mack, J. Sturtevant, J. D. Byers and D. A. Miller, *Proc. SPIE*, **2438**, (1995), 167.